Testing post-IR IRSL luminescence dating methods in the southwest Mojave Desert, California, USA

Andrew S Carr[1]*, Alex S Hay[1]*, Mark Powell[1], Ian Livingstone[2]

1: School of Geography, Geology and the Environment, University of Leicester, University Road, Leicester LE1 7RH, UK
2: The Graduate School, University of Northampton, Northampton, NN2 7AL, UK

*corresponding authors asc18@le.ac.uk and ash24@le.ac.uk

Abstract

The Mojave Desert presents an array of Pleistocene lacustrine deposits and aeolian landforms to which, at times, it has proved challenging to apply luminescence methods. We tested the suitability of K-feldspar post-IR IRSL methods using two sites with independent radiocarbon dating – shorelines at Harper Lake and Silver Lake – considering: 1) overall performance of the post-IR IRSL 225°C ($pIRIR_{225}$) protocol, 2) effect of test dose size on $pIRIR_{225}$ D_e, 3) anomalous fading correction of $pIRIR_{225}$ ages; 4) preliminary single grain $pIRIR_{225}$ results.

We observe consistently good performance of the single aliquot $pIRIR_{225}$ protocol, with good dose recovery, acceptable recycling ratios, low recuperation and low inter-aliquot scatter. The $pIRIR_{225}$ ages for Silver Lake (8.8 ± 0.4 and 11.3 ± 0.5 ka) and Harper Lake (both 25.4 ± 1.4 ka) are in substantially better agreement with the independent dating than low temperature (50°C) IRSL and quartz OSL ages. $pIRIR_{225}$ fading rates are reduced to ~2.0-2.5% per decade, but there remains a tendency for under-estimation when using uncorrected ages. A need for fading correction is further implied at Harper Lake via comparison with multi-elevated temperature (MET)-PIR age plateaus and $pIRIR_{290}$ measurements, although at the younger Silver lake site these methods produce ages nearly identical to the uncorrected $pIRIR_{225}$ ages. Preliminary single grain $pIRIR_{225}$ measurements suggest a ~25-30% usable grain yield. At Silver Lake the single grain and single aliquot ages agree well despite over-dispersion of the single grain equivalent dose distribution. At Harper Lake the single grain and single aliquot $pIRIR_{225}$ ages also agree well, although a population of insensitive, lower D_e grains is observed. These grains are not associated with significantly higher fading rates.

Introduction

The Mojave Desert (southwest USA) preserves abundant evidence for Pleistocene palaeo-lakes (Enzel et al., 2003) and relict aeolian deposits (Lancaster and Tchakerian, 1996). Various luminescence dating methods have been applied, including quartz optically stimulated luminescence (OSL) (Bateman et al., 2012; Fuchs et al., 2015), K-feldspar thermoluminescence (TL) and infra-red stimulated luminescence (IRSL; Clarke et al. 1995; Rendell and Sheffer, 1996). Presently there are conflicting ages between studies (e.g. Rendell and Sheffer, 1996 and Bateman et al., 2012), within sites (stratigraphic inversions), and contrasting results compared to independent dating (e.g. Owen et al., 2007). Quartz may be an unreliable dosimeter in the Mojave due to its low sensitivity and a contaminating K-feldspar signal (Lawson et al., 2012). K-feldspar is, however abundant in Mojave sediments and is a potentially advantageous mineral choice given the relatively high environmental dose rates (typically > 3 Gy ka^{-1}). Previous applications of K-feldspar IRSL (Rendell and Sheffer, 1996) did not include anomalous fading correction and subsequent studies using low temperature IRSL have reported variable, but sometimes high fading rates (Garcia et al., 2014).

We consider the reliability of K-feldspar ages derived via post-IR IRSL (pIRIR) methods, which can isolate a slower (or non) fading IRSL signal (Thomsen et al., 2008; Buylaert et al., 2012). Demonstrating the suitability of pIRIR approaches would be an important step in improving chronological control in the Mojave, and recent applications have shown promise (McGuire and Rhodes, 2015; Roder et al., 2012). We sampled two sites with independent dating to consider pIRIR protocol performance.

Study sites

Two palaeo-lakes in the Mojave River catchment were analysed; Harper Lake and Silver Lake (**Figure 1**). Sourced in the San Bernardino Mountains to the southwest, the Mojave River experienced episodes of perennial flow during the Pleistocene, periodically maintaining Lake Manix, Harper Lake and the downstream Silver Lake. This catchment history is discussed elsewhere (Meek, 1999; Enzel et al., 2003; Wells et al., 2003; Reheis et al., 2012; 2015).

Silver Lake formed part of pluvial Lake Mojave (Wells et al., 2003) (**Figure 1a; 1c**). Several sites demonstrate lake high-stands (following Wells et al., 2003) at ~22-19 cal ka BP (18.4-16.6 ka; "Lake Mojave 1") and ~16.6-13.3 cal ka BP (13.7-11.4 ka; "Lake Mojave 2"), with intermittent inundation at 13.3-9.8 cal ka BP (~11.4-8.7 ka). A spit-shoreline complex at "Silver Quarry" (Ore and Warren, 1978) was subject to a detailed investigation combining radiocarbon dating of the freshwater bivalve *Anodonta californiensis*, quartz OSL and fine-grain K-feldspar IRSL Multi-Aliquot Additive Dose (MAAD) methods (Owen et al., 2007). Our luminescence samples were obtained from Owen et al.'s (2007) LithoFacies Associations (LFA) LFA8 (SL14-1**;** 0.4 m) and LFA6 (SL14-2**;** 1.2 m) (**Figure 1c**). Using the BCal Bayesian analysis software (**Table S2**), Owen et al. (2007) assigned age ranges of 12.1-11.6 cal ka BP to LFA 8 (7 dates) and 12.2-12.5 cal ka BP to LFA 6 (2 dates). Their quartz OSL ages for LFA 8 (SL125) and LFA6 (SL126) were 6.6 ± 0.7 ka and 6.5 ± 0.6 ka respectively.

Harper Basin (**Figure 1a**) is presently isolated from the Mojave River, but was likely fed by periodic Mojave River avulsions (Meek, 1999). Lake beds are exposed at 'Mountain View Hill' where radiocarbon dates from *A. californiensis* shells of 24,055-33,059 cal yr. BP (24,440 ± 2190 ^{14}C yr BP) and 28,375-29,790 cal yr. BP (25,000 ± 310 ^{14}C yr. BP) were first reported (with a third infinite age; Meek, 1999). Garcia et al. (2014) presented eight new *A. californiensis* radiocarbon dates and luminescence ages from coarse-grain (125-150 µm) post-IR quartz SAR and fine grain (4-11 µm) K-feldspar MAAD IRSL (**Figure 1b**). The new radiocarbon dates ranged from 33,410 to 39,788, cal yr. BP; **Table S2; Figure 1b**), with fading-corrected IRSL ages of 28 ± 2 ka to 46 ± 3 ka (7.2% per decade fading rate). The quartz ages were substantially younger (17-19 ka). Garcia et al. (2014) argued for a probable age of 40-45 ka, but there is variability within and between the radiocarbon and IRSL ages, with the former close to the limits of the method. The independent dating control at Harper Lake is thus less firm than Silver Lake. We sampled the same section and took samples from the beach unit (figure 5 of Garcia et al., 2014) at 0.84 and 1.25 m (**Figure 1c**).

Methods

180-250 µm quartz and K-feldspar grains were isolated, with K-rich feldspars obtained via density separation at 2.58 g cm^{-3} and etched in 10% HF for 10 minutes. All samples were analysed on a Risoe DA20 TL/OSL reader, with quartz luminescence detected through a Hoya U340 filter and IRSL through Schott BG39 and Corning 7-59 filters. Quartz equivalent doses on 2 mm aliquots were determined using the single aliquot regeneration (SAR) protocol (Murray and Wintle, 2000) employing post-IR (50°C) blue LED (125°C) stimulation. 2 mm aliquots of K-feldspar were analysed using a pIRIR protocol comprising a 50°C IRSL stimulation and a subsequent 225°C stimulation (henceforth $pIRIR_{225}$) with a 250°C preheat (1 minute). Anomalous fading rates were determined following Auclair et al. (2003) with corrections following Huntley and Lamothe (2001), using the R package "Luminescence" (Kreutzer et al., 2012).

Dose rates were determined using *in-situ* gamma spectrometry and ICP-MS (**Table S1**). We used the estimated water contents of Owen et al. (2007) and Garcia et al. (2014) (10 ± 5 % and 14.5 ± 5% respectively). A 5 % absolute change in water content produces an age difference of 200-300 years at Silver Lake and ~380 years at Harper Lake.

Results

Silver Lake

$pIRIR_{225}$ ages (**Table 1 and Figure S1)** were obtained using a moderate (23% of D_e) test dose. Sample SL14-1 (LFA8) produced a fading-uncorrected $pIRIR_{225}$ age of 8.8 ± 0.4 ka, and sample SL14-2 (LFA6) an age of 11.3 ± 0.5 ka. The $pIRIR_{225}$ residual D_es following 48 hours of (UK) daylight were 0.8 and 1.0 Gy. A quartz OSL age of 5.2 ± 0.5 ka for SL14-1 (LFA8) is comparable to that of Owen et al. (2007) and is much younger than the radiocarbon dates. All quartz aliquots are rejected if the fast ratio criterion (average ratio 2.4 ± 1.7) is applied (Durcan and Duller, 2011) and in light of the signal contamination

test results (**Figure S2,** after Lawson et al. 2012;) this age is considered unreliable. We infer this probably also applies to Owen et al.'s (2007) quartz ages.

The $pIRIR_{225}$ ages are in better agreement with the radiocarbon dating (BCal ages 12.1-11.6 cal yr. BP and 12.5-12.2 cal. yr BP for LFA8 and LFA6). They show low D_e over-dispersion (3-6%; **Figure S1**), good dose recovery (ratios 1.00 ± 0.01 (SL14-1) and 0.99 ± 0.01 (SL14-2)), low recuperation (<2 % for all aliquots) and recycling ratios consistent with unity (e.g. SL14-1 average 1.02 ± 0.02). The SL14-1 fading-uncorrected $pIRIR_{225}$ age is younger than the LFA8 BCal radiocarbon age range, although it is within uncertainties of the youngest radiocarbon date from this LFA (AP9; 9081-9322 cal. yr BP; **Table S2; Figure S4**). SL14-2 is within 2 sigma uncertainties of the LFA6 BCal age (12.2-12.5 ka). Thus, although both $pIRIR_{225}$ ages show better agreement with the independent dating, it is prudent to consider possible underestimation relative to the radiocarbon dating.

Test dose size

Test dose size has been shown to impact sample D_e within pIRIR protocols (Li et al., 2014; Lui et al., 2016; Yi et al., 2016; Colarossi et al., 2018). At Silver Lake the natural D_e was determined for test doses between 4 and 65% of the expected D_e (**Figure 2**). The results suggest possible age underestimation at low test doses (but note the uncertainties), with a much clearer tendency at high doses. Moderate (23-30% of D_e) test doses produced ages closest the expected age. Considering the dose response curves (DRC) for low (3.8%), moderate (27% of D_e) and high (65% of D_e) test doses (**Figure S3**), low test dose DRCs saturate faster (D_0= ~43 Gy compared to > 150 Gy for 27% test dose), with little difference between moderate and high test doses. The age difference between moderate and high test doses seems to reflect a lower Ln/Tn for the latter. The test dose used for the age estimates in **Table 1** (23%) is thus unlikely to be a source of age-underestimation.

Ages and fading rates

The $pIRIR_{225}$ fading rates are 2.1 ± 0.3% and 0.7 ± 0.3% per decade for SL14-1 and SL14-2 and fading correction brings them into better (SL14-1) and very good (SL14-2) agreement with the radiocarbon ages (**Table 1; Figure S4**). The fading rates for the IR 50°C are 6.5 ± 0.3% and 5.6 ± 0.4% for SL14-1 and SL14-2, but with fading-correction (10.3 ± 0.6 and 12.4 ± 0.8 ka) they show good correspondence with the fading-corrected $pIRIR_{225}$ and radiocarbon ages.

The need for fading correction of the post-IR IRSL signal may be removed by using a higher temperature second IR stimulation ($pIRIR_{290}$; Buylaert et al., 2012). This is usually at the expense of a larger unbleached/residual IRSL signal (Kars et al., 2014) and in water-lain deposits, it may be advantageous to utilise a more easily bleached signal (i.e. $pIRIR_{225}$). To assess this further, we compared the $pIRIR_{225}$ ages and independent ages with the $pIRIR_{290}$ (Buylaert et al., 2012) and multiple elevated temperature (MET) PIR (Li and Li, 2011) methods. For sample SL14-1, we observe possible MET-PIR plateau above 200°C, but the 250°C age (8.8 ± 0.5 ka) matches the fading-uncorrected $pIRIR_{225}$ age (**Figure 3**). Although $pIRIR_{290}$ and MET-300°C data are broadly within this range, they show more inter-aliquot scatter, perhaps indicating the unsuitability of higher preheating/stimulation temperatures. Increasing the first stimulation temperature (for $pIRIR_{225}$) to 80°C or 110°C increases the age of SL14-1 to 9.9 ± 0.4 and 9.7 ± 0.4 ka, perhaps implying removal of a fading-prone signal. However, the trend does not continue with higher (180°C) first stimulation temperatures (8.7 ± 0.5 ka). Thus, the MET-PIR 250°C age, $pIRIR_{290}$ and the uncorrected $pIRIR_{225}$ age for SL14-1 all fall at the lower edge of the expected BCal age range (**Figures 3 and S4**) and it is presently unclear whether the MET plateau represents a non-faded age.

Single grain analysis

The single aliquot data show limited inter-aliquot scatter, but given potential signal averaging for K-feldspars (Trauerstein et al. 2014) and the lacustrine context, preliminary single grain measurements were conducted for SL14-1. Grains were mounted on single aliquot disks and stimulated with the IR LED. A dose recovery experiment was conducted, comprising room temperature IR bleaching for 200

seconds and a 33 Gy dose. Of 96 analysed, 22 grains produced acceptable signals (test dose > 3 sigma above background, recycling ratios between 0.8 and 1.2, recuperation < 5%). The central age model (CAM) dose recovery ratio was 1.02 ± 0.03 (identical to arithmetic mean). The D_e over-dispersion from the dose recovery experiment was low at 3.3 ± 0.4% (cf. Rhodes, 2015; Brown et al., 2015). This OD was added to the individual grain D_e uncertainties for analysis of the natural D_e. A natural equivalent dose was derived from 21 grains (of 96 measured). The data show significant (37 ± 6 %) over-dispersion, but the CAM-derived age (8.9 ± 0.9 ka) is identical to the single aliquot result (**Figure 4**). The distribution of grain brightness (**Figures 4 and S5**) is skewed (50% of light sum from 18% of grains), but there is no relationship between grain sensitivity and equivalent dose (c.f. Rhodes, 2015), nor is there a correlation between grain fading rates and equivalent dose.

Harper Lake

Harper Lake produced two identical $pIRIR_{225}$ ages (test dose 10% of D_e) of 25.4 ± 1.4 ka (**Table 1; Figure S1**). The fading-uncorrected ages are within uncertainties of one of Meek's (1999) radiocarbon ages, lower than all other radiocarbon ages, and within uncertainties of one fine-grain IRSL age (28 ± 2 ka) (Garcia et al., 2014; **Figure S6**). $pIRIR_{225}$ data show good dose recovery (0.98 ± 0.01 (HL14-1) and 0.97 ± 0.01 (HL14-2)), good recycling ratios (averages 1.01 ± 0.02 and 1.02 ± 0.02) and low recuperation (all aliquots < 0.5%). Residuals following 48 hours of daylight were 5.5 and 3.5 Gy. The 50°C IR ages are 13.0 ± 0.7 ka and 13.9 ± 0.8 ka. Quartz performance was poor (**Figures S2 and S6**) with most aliquots rejected for excessive recuperation (average ~13%) using late background subtraction. A quartz age for HL14-1 from 3 acceptable aliquots using early background subtraction was 25.7 ± 4.4 ka, and 23.6 ± 2.8 ka for the single acceptable aliquot using late background subtraction.

Test dose size

For Harper Lake, the effect of test dose size was investigated with a dose recovery experiment and using the natural IRSL D_e (**Figure 2**). The natural measurements show little sensitivity to test dose size, but the lowest test dose (2.5%) produced significant inter-aliquot scatter. The dose recovery

experiment suggests underestimation at test doses >30% of D_e, with a relatively low test dose (8%) giving the best dose recovery (0.98 ± 0.01; n=3). For both the natural and dose recovery measurements, the DRCs behave as per Silver Lake, with faster saturation for the lowest test doses (D_0 of 100 ± 3 Gy for the 2.5% test dose vs. 306 ± 52 Gy for 48% test dose) and indistinguishable DRCs for moderate (23%) and high (65%) test doses (**Figure S3**). Despite this, lower test doses produced the best dose recovery, with a tendency for lower Ln/Tn ratios rather than a changing DRC at high test doses. The latter was not observed in the natural D_e measurements.

Fading rates

The 50°C IR fading rates are 10.6 ± 2.0 % and 9.4 ± 1.0 % per decade for HL14-1 and 14-2, resulting in large uncertainties with fading-correction. The $pIRIR_{225}$ fading rates are comparable to Silver Lake (2.0 ± 0.4 and 2.4 ± 0.2 %), but the MET-PIR plateau for HL14-2 more unambiguously implies a need for fading correction (**Figure 3**), with the 250°C age of 35.4 ± 2.5 ka within uncertainties of several of Garcia et al.'s (2014) radiocarbon ages (**Figure S6**). The $pIRIR_{290}$ ages are comparable to this (33.4 ± 1.9 ka and 37.3 ± 2.3 ka for HL14-1 and HL14-2 respectively; **Figures 3 and S6**), although the $pIRIR_{290}$ dose recovery results for HL14-1 (1.07 ± 0.05 n=2) (natural dose plus a 66.5 Gy dose) hint at potential overestimation. The fading-corrected $pIRIR_{225}$ ages for both HL14-1 and HL14-2 are 29.0 ± 1.9 ka and 29.8 ± 2.0 ka, placing them good agreement with Meek's (1999) radiocarbon ages, but still somewhat lower than Garcia et al.'s (2014) radiocarbon ages (**Figure S6**) and most of their IRSL ages.

Single grain analysis

28 of 96 grains from HL14-1 produced acceptable luminescence characteristics. The distribution of grain brightness (**Figure S5**) is skewed (~20% of grains account for 50% of the light sum) and the equivalent dose distribution is over-dispersed (29 ± 4%, with 3.3% added to individual uncertainties). A cluster of lower D_e grains are also insensitive (**Figure 4**), but are not associated with higher fading rates (**Figure S7**). The CAM D_e using all grains is 94.0 ± 6.2 Gy, but increases to 112.4 ± 6.1 Gy when

the brightest 50% are used (n=14), and the D_e distribution becomes less dispersed (OD 16 ± 4%). The (fading uncorrected) age using the brightest grains (26.8 ± 1.9 ka) is indistinguishable from the single aliquot age. Individual grain fading rates range from 11% to -6% per decade. Although the uncertainties are large, the mean is comparable to the single aliquot analysis (2.8 % per decade).

Discussion

Comparison with independent dating is limited by several factors. For Harper Lake there are inconsistencies between the radiocarbon chronologies of Meek (1999) and Garcia et al. (2014). Garcia et al.'s (2014) preferred site age was older still at 40-45 ka (citing palaeosol ages in the down-catchment Lake Manix Basin (Reheis et al., 2012) and noting that post-depositional contamination would tend to make radiocarbon ages too young; see also Reheis et al., 2015). However, the precise reasons remain unclear, and the spread of ages makes interpretation difficult (Reheis et al., 2015). The impact of the hard-water effect on radiocarbon ages was suggested by Owen et al. (2007) to be < 150 years, although Berger and Meek (1992) reported offsets up to 450 years. For luminescence ages there are also potential offsets from water content estimation. Using water contents at saturation (~35%) or akin to the modern values (2 %) results in $pIRIR_{225}$ ages of 8.5-9.6 ka for SL14-1/LFA8 and 23.8-27.8 ka for HL14-1. Given these are extreme values, it is unlikely that this alone accounts for any differences (for Harper Lake particularly).

Nonetheless, the $pIRIR_{225}$ ages show substantially better agreement with the independent dating than the 50°C IR and quartz OSL ages (**Table 1; Figures S4 and S6**). The single aliquot $pIRIR_{225}$ data are highly reproducible and an absence of overestimation at either site implies incomplete bleaching is not an issue, despite the lacustrine contexts. Lower 50°C IR ages reflect a need for anomalous fading correction (noting the inter-site variability) (**Table 1**), while quartz underestimation reflects low sensitivity and (probably) a significant contaminating non-quartz signal (**Figure S2**). At Harper Lake a small proportion of quartz aliquots produce ages in better agreement with the $pIRIR_{225}$ ages with early background signal subtraction or if the fast ratio (Durcan and Duller,

2011) is employed as screening methods (Hay, 2018). The aliquot rejection rate is high and the ages are still lower than the fading-corrected $pIRIR_{225}$ ages, and much of the independent chronology. Quartz ages not employing such rigorous screening (at least, quartz of local origin) should be considered with care.

Limited sensitivity of the natural D_e to test dose size is observed for test doses between 5 and ~56% of D_e at Harper Lake and between 5 and 30% at Silver Lake. There is a clear impact on the DRC for very small test doses (**Figure S3**), but this does not result in consistently higher or lower D_e estimates (note the scatter for the low test doses for the Harper Lake natural signal; Lui et al., 2016). At Harper Lake the dose recovery data appear more sensitive to test dose than the natural D_e data (Yi et al., 2016). There is a significant correlation between Lx background and the Tx initial signals for all test dose analyses (Colarossi et al., 2018), and the slope of this relationship increases at higher test doses. There is a tendency towards poorer dose recovery at high test doses at Harper Lake. This is due to a lower Ln/Tn (**Figure S3**), which is also seen in natural D_e data at Silver Lake. The reason(s) for this is(are) not clear, but it implies an effect on the initial natural dose/test dose measurement.

At Silver Lake the fading-uncorrected $pIRIR_{225}$ ages are close(SL14-2) or fall below (14-1) the radiocarbon age ranges. For SL14-1 especially this implies fading correction (2.1% per decade) is necessary (**Table 1**). The MET-PIR data do not unambiguously support this however, although a small increase in the first stimulation temperature does increase the sample age. At Harper Lake most results from the independent dating and the MET-PIR / $pIRIR_{290}$ data more strongly indicate that fading correction of the $pIRIR_{225}$ ages (2.0-2.4% per decade) is required. The MET-PIR plateau (200-250°C) and $pIRIR_{290}$ data fall within the lower range of Garcia et al.'s (2014) radiocarbon dates. The fine-grain MAAD IRSL ages (*ibid*) show less consistency than our coarse-grain $pIRIR_{225}$ and $pIRIR_{290}$ ages (samples ALG-HL-OSL2 vs ALG-HL-OSL3 in Garcia et al., 2014), which perhaps reflects uncertainty imparted when correcting the former for the high 50°C IR fading rates at this site (**Table 1**), which was also based on fading analysis of a single sample.

The preliminary single grain data indicate (from dose recovery data) rather low "intrinsic" over-dispersion (using the IR LED), but this requires further investigation (c.f. Rhodes, 2015). The limited number of grains should be kept in mind. There is variability in both the signal contribution from individual grains (**Figure S5**) and in the presence of a "declining baseline" (i.e. systematically lower D_es for the dimmest grains; Rhodes, 2015; **Figure 4; Figure S7**). At Harper Lake using the brightest grains reduces OD and moves the resulting age closer to the independent dating (Lamothe et al., 2012), but the result is still within uncertainties of the age obtained using all the grains. Such a relationship is not seen at Silver Lake. At Harper Lake the insensitive, lower D_e grains do not have higher fading rates (**Figure S7**). The internal K/Rb contents of the grains were not assessed, but some studies suggest that K content may not be strongly associated with grain sensitivity (Smedley et al., 2012) or fading rate (Trauerstein et al., 2014).

Conclusions

The $pIRIR_{225}$ protocol shows significantly better agreement with independent dating than the 50°C IR and quartz OSL ages in the Mojave region studied. Quartz consistently and significantly underestimates expected sample ages. At both sites the $pIRIR_{225}$ ages show improved agreement with the independent dating after fading correction, with the MET-PIR and $pIRIR_{290}$ results showing even better agreement with independent ^{14}C ages (of Garcia et al., 2014) at Harper Lake. However, this is not always the case, as at the younger Silver Lake site the SL14-1 MET-PIR and $pIRIR_{290}$ ages are identical to the uncorrected $pIRIR_{225}$ age. The $pIRIR_{225}$ measurements show limited sensitivity to test dose size at Harper Lake, but at both sites the DRCs saturate faster for low test doses and underestimate for high test doses at Silver Lake. The latter is not observed at Harper Lake where the dose recovery data seem to be more sensitive to test dose size than the natural D_e measurements. Contrasting single grain behaviors are also observed, notably in the presence of less sensitive, lower D_e grains at Harper Lake. This mirrors some previous work in suggesting, at least for some sites, that the brightest K-feldspar grains may provide a better estimate of burial dose.

Acknowledgments

ASH was supported by NERC studentship 1358108. Rob Fulton, Jason Wallace and Simon Benson are thanked for logistical support. An anonymous reviewer is thanked for very constructive comments.

References

Auclair, M., Lamothe, M. Huot, S. 2003. Measurement of anomalous fading for feldspar IRSL using SAR. Radiation Measurements 37, 487-492.

Bateman, M.D., Bryant, R.G., Foster, I.D.L., Livingston, I. Parsons, A.J. 2012. On the formation of sand ramps: A case study from the Mojave Desert. Geomorphology 161-162, 93-109.

Berger, R., Meek, N. 1992. Radiocarbon dating of *Anodonta* in the Mojave River basin. Radiocarbon, 34, 578-584.

Brown, N.D., Rhodes, E.J., Antinao, E.V., McDonald, E.V. 2015. Single grain post-IR IRSL signals of K feldspar of alluvial fan deposits in Baja California Sur, Mexico. Quaternary International 362, 132-138.

Buylaert, J-P., Jain, M., Murray, A.S., Thomsen, K.J., Theil, C. Sohbati, R. 2012. A robust feldspar luminescence dating method for Middle and Late Pleistocene sediments. Boreas 41, 435-451.

Colarossi, D., Duller, G.A.T., Roberts, H.M. 2018. Exploring the behaviour of luminescence signals from feldspars: Implications for the single aliquot regenerative dose protocol. Radiation Measurements. 109, 34-44.

Clarke, M.L., Richardson, C.A., Rendell, H.M., 1995. Luminescence dating of Mojave Desert sands. Quaternary Science Reviews 14, 783-789.

Durcan, J.A., Duller, G.A.T. 2011. The fast ratio: A rapid measure for testing the dominance of the fast component in the initial OSL signal from quartz Radiation Measurements 46, 1065-107.

Enzel, Y., Wells, S.G. Lancaster, N. 2003. Late Pleistocene lakes along the Mojave River, southeast California. Geological Society of America, Special Papers, 368 pp.61-78.

Fuchs, M., Dietze, M., Al-Qudah, K., Lomax, J. 2015. Dating desert pavements – first results from a challenging environmental archive. Quaternary Geochronology 30, 342-349.

Garcia, A.L., Knott, J.R., Mahan, S.A., Bright, J. 2014. Geochronology and paleoenvironment of pluvial Harper Lake, Mojave Desert, California, USA. Quaternary Research 81, 305-317.

Hay, A.S. 2018. The influence of complex topography on aeolian sediment accumulation and preservation: an investigation of morphology and process history. Unpublished PhD thesis, University of Leicester.

Huntley, D.J., Lamothe, M. 2001. The ubiquity of anomalous fading in K-feldspars and the measurement and correction for it in optical dating. Canadian Journal of Earth Science 38, 1093-1106.

Jefferson, G.T. 2003. Stratigraphy and palaeontology of the middle and late Pleistocene Manix Formation, and paleoenvironments of the central Mojave River, southern California. Geological Society of America, Special Papers, 368, 43-60.

Kars, R.H., Reimann, T., Wallinga, J. 2014. Are feldspar SAR protocols appropriate for post-IR IRSL dating? Quaternary Geochronology 22, 126-136.

Kreutzer, S., Schmidt, C., Fuchs, M.C., Dietze, M., Fisher, M., Fuchs, M. 2012. Introducing an R package for luminescence dating analysis. Ancient TL 30, 1-7.

Lamothe, M., Barré, M., Huot, S., Ouimet, S. 2012. Natural luminescence and anomalous fading in K-feldspar. Radiation Measurements 47, 682-687.

Lancaster, N., Tchakerian, V.P. 1996. Geomorphology and sediments of sand ramps in the Mojave. Geomorphology 17, 151-165.

Lawson, M.J., Roder, B.J., Stang, D.M., Rhodes, E.J. 2012. OSL and IRSL characteristics of quartz and feldspar from southern California, USA. Radiation Measurements 47, 830-836.

Li, B., Li S-H. 2011. Luminescence dating of K-feldspar from sediments: A protocol without anomalous fading correction. Quaternary Geochronology 6**,** 468-479.

Li, B., Jacobs, Z., Roberts, R.G. Li, S-H. 2014. Review and assessment of the potential of post-IR IRSL dating methods to circumvent the problem of anomalous fading in feldspar luminescence. Geochronometria 41, 178-201.

Lui, J., Murray, A.S., Sohbati, R., Jain, M. 2016. The effect of test dose and first IR stimulation temperature on post-IR IRSL measurements of rock slices. Geochronometria 43, 179-187.

McGuire, C., Rhodes, E.J. 2015. Determining fluvial sediment virtual velocity on the Mojave River using K-feldspar IRSL: Initial assessment. Quaternary International 362, 124-131.

Meek, N. 1999. New discoveries about the Late Wisconsinan history of the late Mojave River system. San Bernadino County Museum Association Quarterly 46, 113-117.

Murray, A.S. Wintle, A.G. 2000. Luminescence dating of quartz using an improved single-aliquot regenerative-does protocol. Radiation measurements 32, 57-73.

Ore, H.T., Warren, C.N. 1978. Late Pleistocene-early Holocene geomorphic history of Lake Mojave, California. Geological Society of America Bulletin 82, 2553-2562.

Owen, L.A., Bright, J., Finkel, R.C., Jaiswal, M.K., Kaufman D.S., Mahan, S., Radtke, U., Schneider J.S., Sharp, W., Singhvi, A.K., Warren, C. 2007. Numerical dating of a Late Quaternary spit-shoreline complex at the northern end of Silver Lake playa, Mojave Desert, California: A comparison of the applicability of radiocarbon, luminescence, terrestrial cosmogenic nuclide, electron spin resonance, U-series and amino acid racemization methods. Quaternary International 166, 87-110.

Reheis, M.C., Bright, J., Lund, S.P., Miller, D.M., Skipp, G., Fleck, R.J. 2012. A half-million-year record of paleoclimate from the Lake Manix Core, Mojave Desert, California. Palaeogeography, Palaeoclimatology, Palaeoecology 365, 11-37.

Reheis, M.C., Miller, D.M., McGeehin, J.P., Redwine, J.R., Oviatt, C.G., Bright, J. 2015. Directly dated MIS 3 lake-level record from Lake Manix, Mojave desert, California, USA. Quaternary Research 83, 187-203.

Rendell, H.M., Sheffer, N.L. 1996. Luminescence dating of sand ramps in the Eastern Mojave Desert. Geomorphology 17, 187-197.

Rhodes, E.J. 2015. Dating sediments using potassium feldspar single-grain IRSL: initial methodological considerations. Quaternary International 362, 14-22.

Roder, B., Lawson, M., Rhodes, E.J. Dolan, J., McAuliffe, L., McGill, S. 2012. Assessing the potential of luminescence dating for fault slip rate studies on the Garlock fault, Mojave Desert, California, USA. Quaternary Geochronology 10, 285-290.

Smedley, R.K., Duller, G.A.T., Pearce, N.J.G., Roberts, H.M. 2012. Determining the K-content of single-grains of feldspar for luminescence dating. Radiation Measurements 47, 790-796.

Thomsen, K.J., Murray, A.S., Jain, M., Bøtter-Jensen L. 2008. Laboratory fading rates of various luminescence signals from feldspar-rich sediment extracts. Radiation measurements 43, 1474-1486.

Trauerstein, M., Lowick, S.E., Preusser, F., Schlunegger, F. 2014. Small aliquot and single grain IRSL and post-IR IRSL dating of fluvial and alluvial sediments from the Pativilca Valley, Peru. Quaternary Geochronology 22, 163-174.

Vermeesch, P. 2009. RadialPlotter: a Java application for fission track, luminescence and other radial plots. Radiation Measurements 44, 409-410

Wells, S.G., Brown, W.J., Enzel, Y., Anderson, R.Y., McFadden, L.D. 2003. Late Quaternary geology and paleohydrology of pluvial Lake Mojave, southern California. Geological Society of America, Special Papers 358. 79-114.

Yi, S., Buylaert, J-P., Murray, A.S., Lu, H., Thiel, C., Zeng, L. 2016. A detailed post-IR IRSL dating study of the Niuyangzigou loess site in northeastern China. Boreas 45, 644-657.

Figure Captions

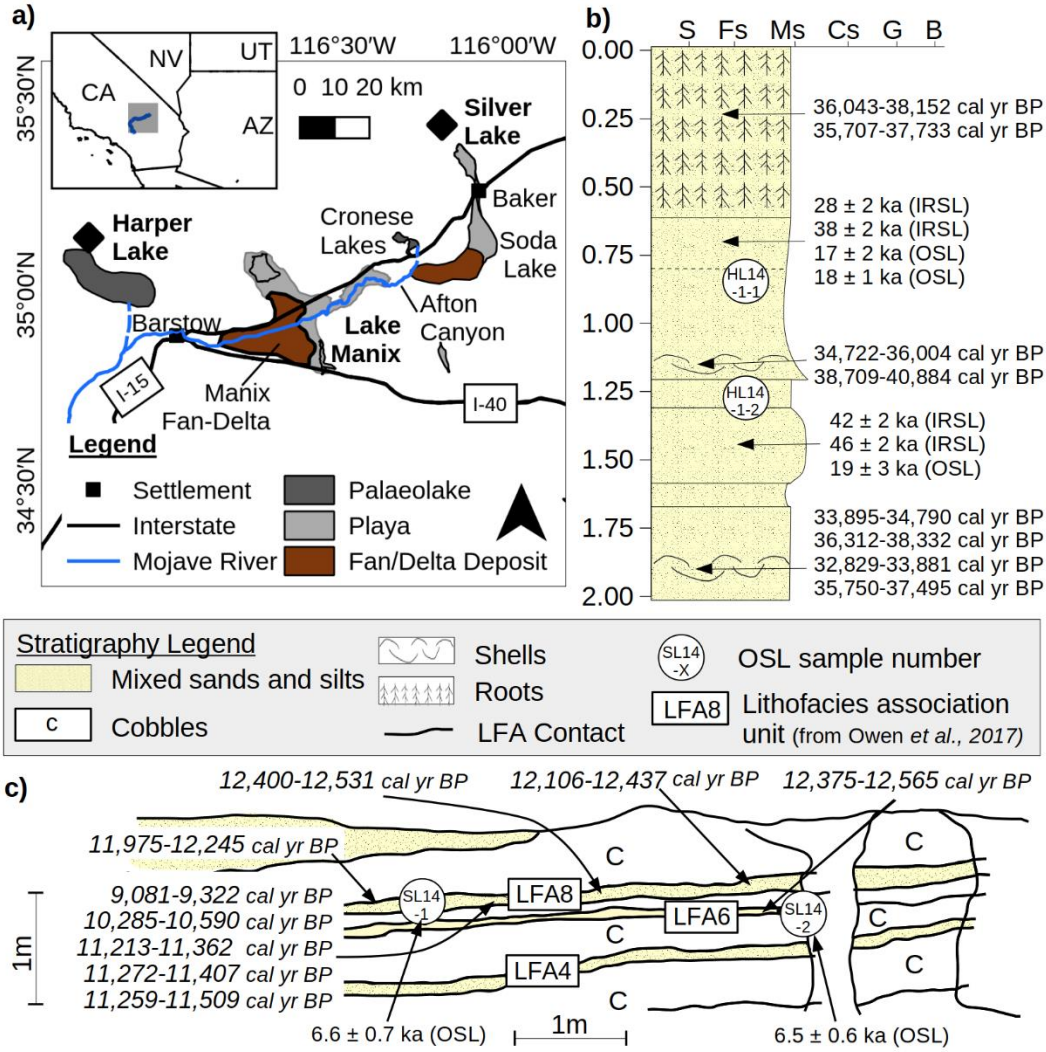

Figure 1: A) Map of the Mojave River catchment, showing the major palaeo-lakes and the present Mojave River course. B) Site stratigraphy with previously published (calibrated) radiocarbon dates and luminescence ages for Harper Lake. C) Silver Lake stratigraphy and calibrated radiocarbon age ranges (modified after Owen et al. 2007).

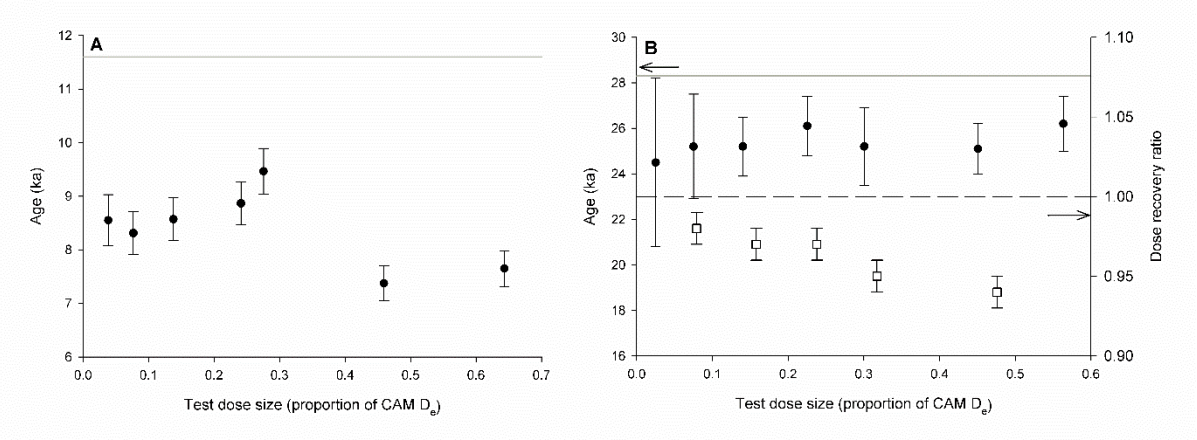

391

392 **Figure 2**: Relationship between test dose size and sample age for (**A**) Silver Lake SL14-1 and (B)
393 Harper Lake HL14-1. In A the horizontal line shows the lower 11.6 ka BCal estimate for LFA8 (see
394 **Table S2**). In **B** the lowest calibrated (median value) radiocarbon age for HL14-1 is shown with a solid
395 line; (Meek, 1999), with the natural luminescence signal as filled circles. The HL14-1 dose recovery
396 results (open squares) are shown on the secondary Y axis and the dashed line marks a dose recovery
397 ratio of 1. Averages and standard deviations of 3 aliquots are shown.

398

399

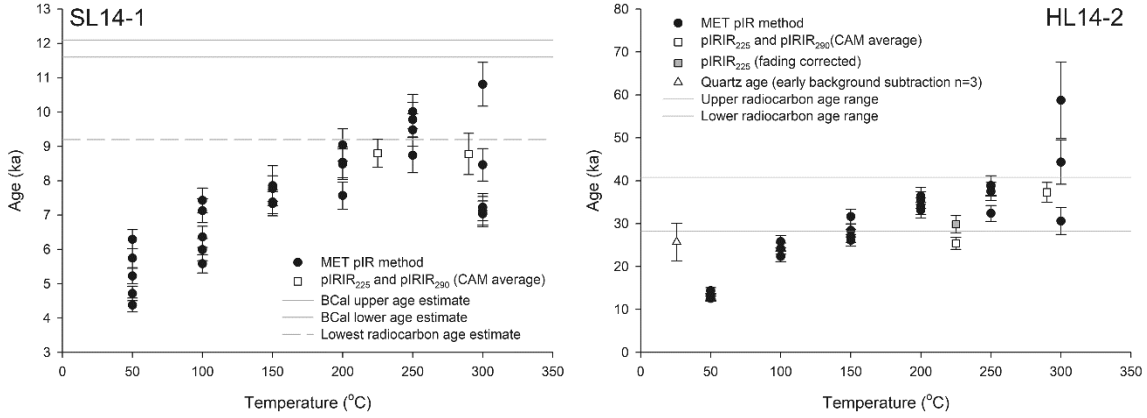

400

401 **Figure 3**: MET-PIR plateaus and $pIRIR_{225}$ and $pIRIR_{290}$ age estimates for samples SL14-1 and HL14-2.
402 The BCal age range is shown for SL14-1 (with the median calibrated age for the youngest sample
403 (AP9) also shown). The range of calibrated radiocarbon ages (median calibrated values in **Table S2**)
404 are plotted for Harper Lake. Note that the Harper Lake quartz age is from sample HL14-1 (**Table 1**).

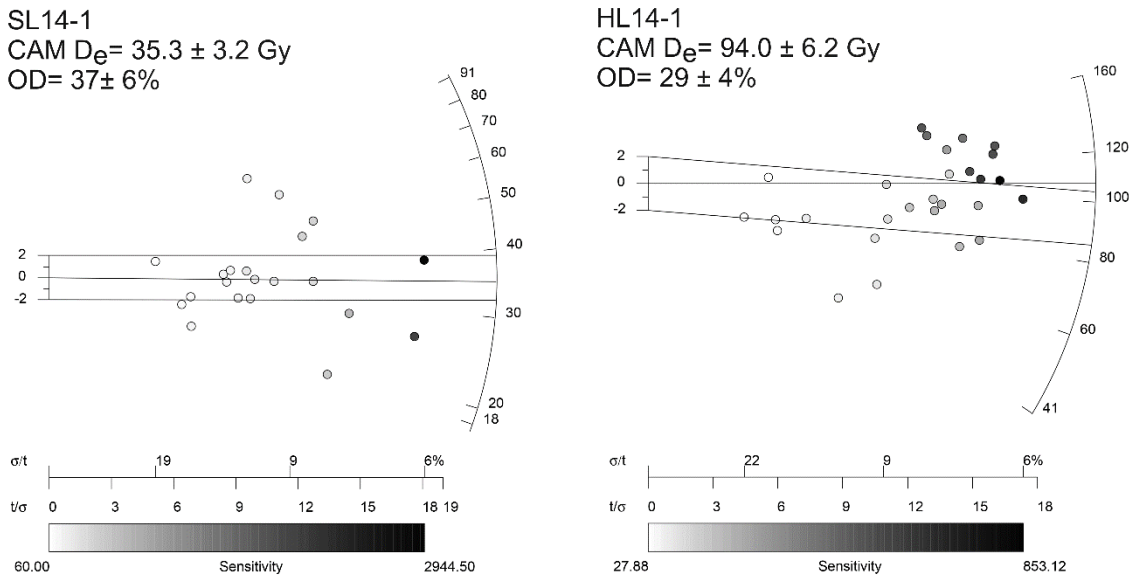

405

406 **Figure 4**: Single grain radial plots (Vermeesch, 2009) for samples SL14-1 and HL14-1. The samples are
407 grey-scaled by sensitivity (first (background subtracted) test dose response in counts s^{-1} Gy^{-1}). For
408 Harper Lake the two sigma lines are centred on the CAM estimate for all accepted grains, with the
409 marker line indicating the single aliquot CAM D_e. Similarly, the marker line for SL1-1 is the single
410 aliquot CAM D_e.

411

412

Table 1: Equivalent doses and associated age estimates for the various K-feldspar IRSL methods and the quartz SAR.

Sample	CAM D_e IR 50 (Gy) (n)	Age IR50 (ka)	Age IR50 (ka) Fading correct	CAM D_e $pIRIR_{225}$ (Gy) (n)	Age $pIRIR_{225}$ (ka)$^{-}$	Age $pIRIR_{225}$ (ka) Fading correct	Single grain CAM D_e $pIRIR_{225}$ (Gy) (n)	Single grain age-$pIRIR_{225}$ (ka)	CAM D_e $pIRIR_{290}$ (Gy) (n)	Age $pIRIR_{290}$ (ka)$^{-}$	CAM D_e Quartz* (Gy) (n)	Age quartz (ka)
SL14-1	25.2 ± 0.95 (20)	**6.36 ± 0.30**	**10.3 ± 0.6**	34.9 ± 1.2 (20)	**8.8 ± 0.4**	**10.1 ± 0.5**	35.3 ± 3.22 (21)	**8.9 ± 0.9**	33.1 ± 1.29 (4)^	**8.4 ± 0.4**	16.3 ± 2.0	**5.2 ± 0.6**
SL14-2	37.4 ± 1.23 (19)	**8.26 ± 0.40**	**12.4 ± 0.8**	51.2 ± 1.6 (19)	**11.3 ± 0.5**	**11.9 ± 0.6**	nd	nd	nd	**nd**	nd	**nd**
HL14-1	54.4 ± 1.91 (22)	**13.0 ± 0.70**	**42.1 ± 20**	107 ± 3.5 (22)	**25.4 ± 1.4**	**29.1 ± 1.8**	94.0 ± 6.2 (28)	**22.4 ± 1.8**[#]	140 ± 4.8 (8)	**33.4 ± 1.9**	85.6 ± 13.8 (3)	**25.6 ± 4.3**
HL14-2	56.9 ± 2.12 (20)	**13.9 ± 0.80**	**34.6 ± 7.8**	104 ± 3.2 (20)	**25.4 ± 1.4**	**29.9 ± 1.8**	nd	nd	152 ± 7.0 (8)	**37.3 ± 2.3**	nd	**nd**

$^{-}$ No residual subtraction was performed

*For Harper Lake the quartz D_e is derived from three acceptable aliquots using early background subtraction

112.4 ± 6.1 Gy and **26.8 ± 1.9 ka** using the brightest 50% of grains

^Excluding high outlier aliquot with D_e/age of 42 Gy/ 10.8 ka (**Figure 3**)

Supplementary material – Carr et al.

Table S1: Details of dose rate determinations

Sample	U (ppm)	Th (ppm)	K (%)	Grain size (μm)	Int. beta dose rate (Gy ka^{-1})	Ext. beta dose rate (Gy ka^{-1})	Gamma dose rate (Gy ka^{-1})	Cosmic dose rate (Gy ka^{-1})	Total dose rate (Gy ka^{-1})
SL14-1	4.08	8.99	1.66	180-250	0.99 ± 0.07	1.54 ± 0.11	1.23 ± 0.48	0.21 ± 0.01	**3.96 ± 0.14**
SL14-2	2.54	14.2	2.16	180-250	0.99 ± 0.07	1.76 ± 0.13	1.60 ± 0.59	0.19 ± 0.01	**4.53 ± 0.16**
HL14-1	1.17	4.52	3.02	180-212	0.85 ± 0.06	1.89 ± 0.20	1.24 ± 0.51	0.21 ± 0.01	**4.19 ± 0.17**
HL14-2	1.97	4.01	2.85	180-212	0.85 ± 0.06	1.86 ± 0.14	1.19 ± 0.48	0.20 ± 0.01	**4.10 ± 0.16**

- Gamma dose rate derived from *in-situ* gamma spectrometry.
- Beta dose rates were derived from ICP-MS of sample tube ends, corrected for grain size following Mejdahl (1979) and Redhead (2002) and water content following Aitken (1985) using element conversion factors of Guerin et al. (2011). Water contents were 10 ± 5% and 14.5 ± 5% following Owen et al. (2007) and Garcia et al. (2014) (respectively). Measured water contents were 0.6-0.8% (Harper Lake) and 1.2-1.9% (Silver Lake).
- U, Th and K contents derived via ICP-MS with relative uncertainties of 10% (U and Th) and 5% (K).
- Internal K and Rb contents were 12.5 ± 0.5 % and 400 ± 100 ppm (Huntley and Baril 1997; Huntley and Hancock, 2001).
- Cosmic dose rates following Prescott and Hutton (1994).

Table S2: Published radiocarbon dates from Owen et al. (2007), Garcia et al. (2014) and Meek (1999) and their calibration using INTCAL13 (Reimer et al., 2013) and CALIB (Stuiver and Reimer, 1993)). The UCLA and UCR codes for Harper Lake relate to Meek (1999).

Sample	Site	Material	^{14}C age (years)	2 sigma calibrated range (cal yr. BP) (probability)	Median age (cal yr. BP)
AP9	Silver Lake LFA8	*Anodonta californiensis* shell	8240 ± 40	9081-9322 (0.92)	9210
AP10	Silver Lake LFA8	*Anodonta californiensis* shell	9290 ± 50	10,285-10,590 (0.98)	10,481
AP11	Silver Lake LFA8	*Anodonta californiensis* shell	9880 ± 40	11,213-11,362 (0.98)	11,271
AP12	Silver Lake LFA8	*Anodonta californiensis* shell	9790 ± 40	11,272-11,407 (0.76)	11,216
AP3	Silver Lake LFA8	*Anodonta californiensis* shell	9970 ± 40	11,259-11,509 (0.79)	11,393
AP5	Silver Lake LFA8	*Anodonta californiensis* shell	10,320 ± 40	11,975-12,245 (0.79)	12,132
AP6	Silver Lake LFA8	*Anodonta californiensis* shell	10,430 ± 40	12,106-12,437 (0.88)	12,310
AP4	Silver Lake LFA6	*Anodonta californiensis* shell	10,420 ± 40	12,400-12,531 (1.00)	12,292
AP1	Silver Lake LFA6	*Anodonta californiensis* shell	10,480 ± 40	12,375-12,565 (0.84)	12,453
ALG-HV-04	Harper Lake Mudflat	*Anodonta californiensis* shell	32,830 ± 370	36,043-38,152 (1.00)	36,927

ALG-HV-07	Harper Lake Mudflat	*Anodonta californiensis* shell	32,580 ± 350	35,707-37,733 (1.00)	36,564
ALG-HV-06	Harper Lake Beach	*Anodonta californiensis* shell	35,230 ± 490	38,709-40,884 (1.00)	39,778
ALG-HV-03	Harper Lake Beach	*Anodonta californiensis* shell	31,440 ± 310	34,722-36,004 (1.00)	35,328
ALG-HV-05	Harper Lake shoreface	*Anodonta californiensis* shell	30,340 ± 260	33,895-34,790 (1.00)	34,342
ALG-HV-02	Harper Lake shoreface	*Anodonta californiensis* shell	33,080 ± 370	36,312-38,332 (1.00)	37,262
ALG-HV-08	Harper Lake shoreface	*Anodonta californiensis* shell	29,210 ± 240	32,829-33,881 (1.00)	33,412
ALG-HV-09	Harper Lake shoreface	*Anodonta californiensis* shell	32,540 ± 300	35,750-37,495 (1.00)	36,483
UCR2867	Harper Lake upper shell horizon	*Anodonta californiensis* shell	25,000± 310	28,375-29,790 (1.00)	29061
UCLA 2627A	Harper Lake upper shell horizon	*Anodonta californiensis* shell	24,440 ± 2190	24,055-33059 (1.00)	28,576

440

441

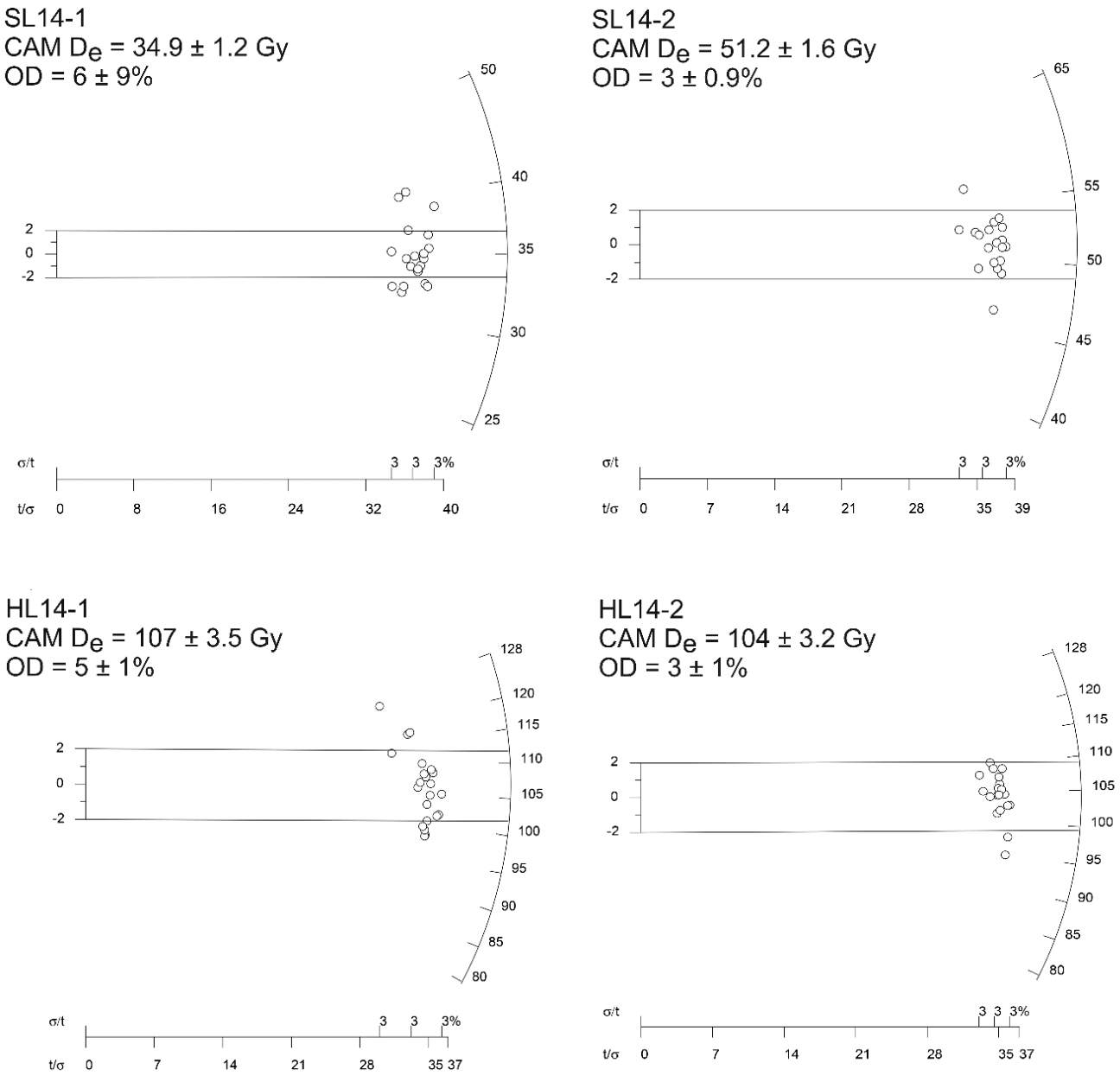

Figure S1: Radial plots for the $pIRIR_{225}$ single aliquot (2 mm) equivalent dose data from Silver and Harper Lake (radial plots were created using the Radial Plotter software of Vermeesch (2009)).

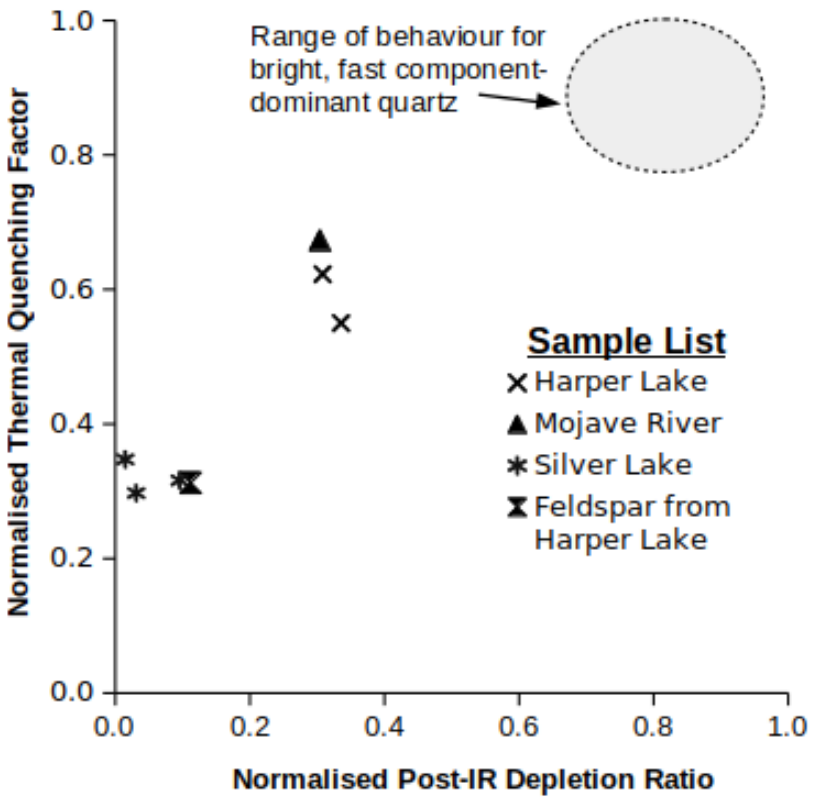

447

448 **Figure S2**: Quartz IR-bleaching and thermal quenching contamination test results (following Lawson
449 et al., 2012) for the Silver Lake and Harper Lake coarse-grained quartz extracts. Also shown is a
450 sample from the modern Mojave River bed (filled triangle) to provide a comparative indication of
451 the behaviour of quartz in the wider Mojave catchment. The grey circle indicates the typical range
452 for quartz extracts with a bright, fast component-dominated quartz OSL signal (samples from
453 numerous locations around the world as analysed in our laboratory).

454

455

456

457

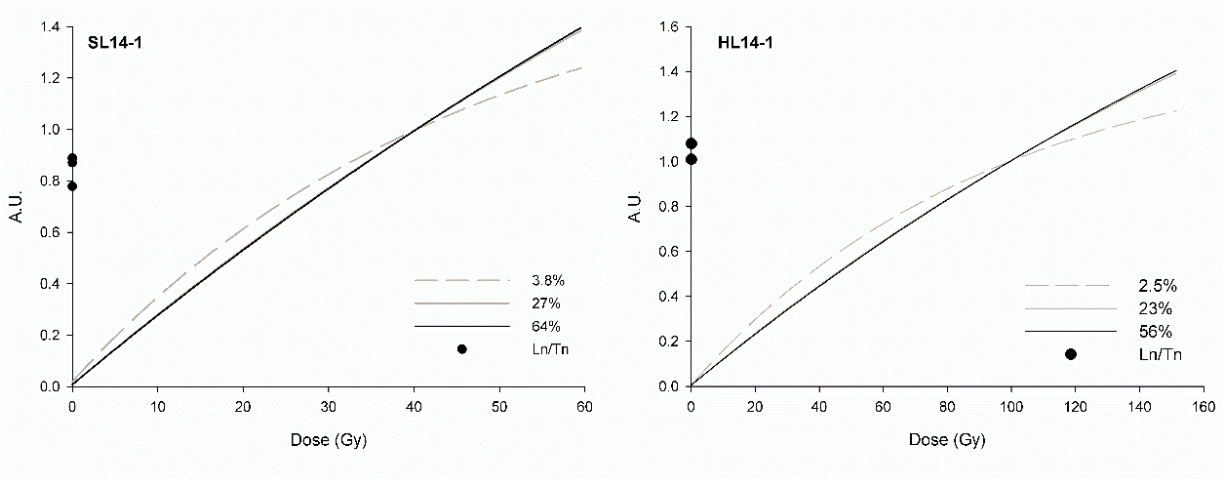

458

Figure S3: The effect of test dose size on dose response curve form, as derived from $pIRIR_{225}$ natural D_e measurement sequences. The data are averages of three aliquots and have been normalised to the 40 Gy (SL14-1) and 90 Gy (HL14-1) regeneration doses. The lower Ln/Tn for the highest test dose at Silver Lake is indicated. At Harper Lake the lower Ln/Tn value relates to the lowest (2.5%) test dose.

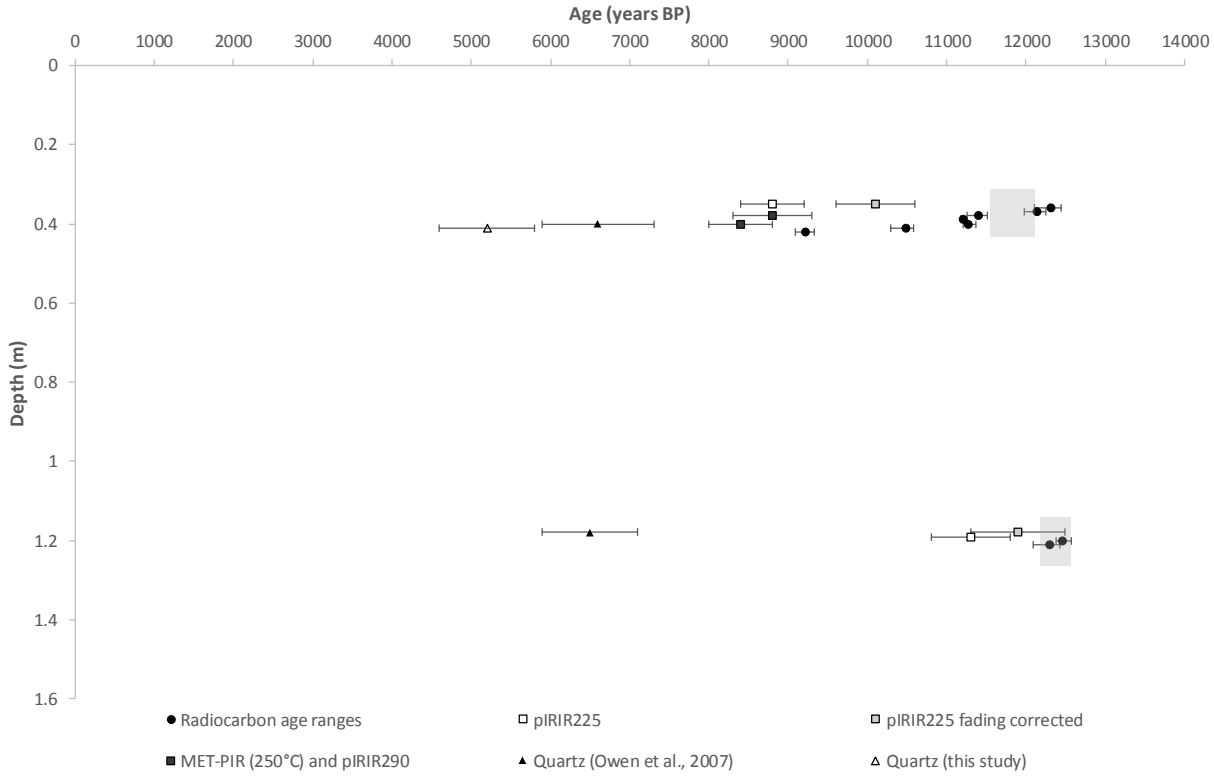

Figure S4: Compared age estimates for the Silver Lake Silver Quarry site LFA 8 and LFA6 as obtained in this study and by Owen et al. (2007). The grey boxes represent the BCal age ranges (*ibid*).

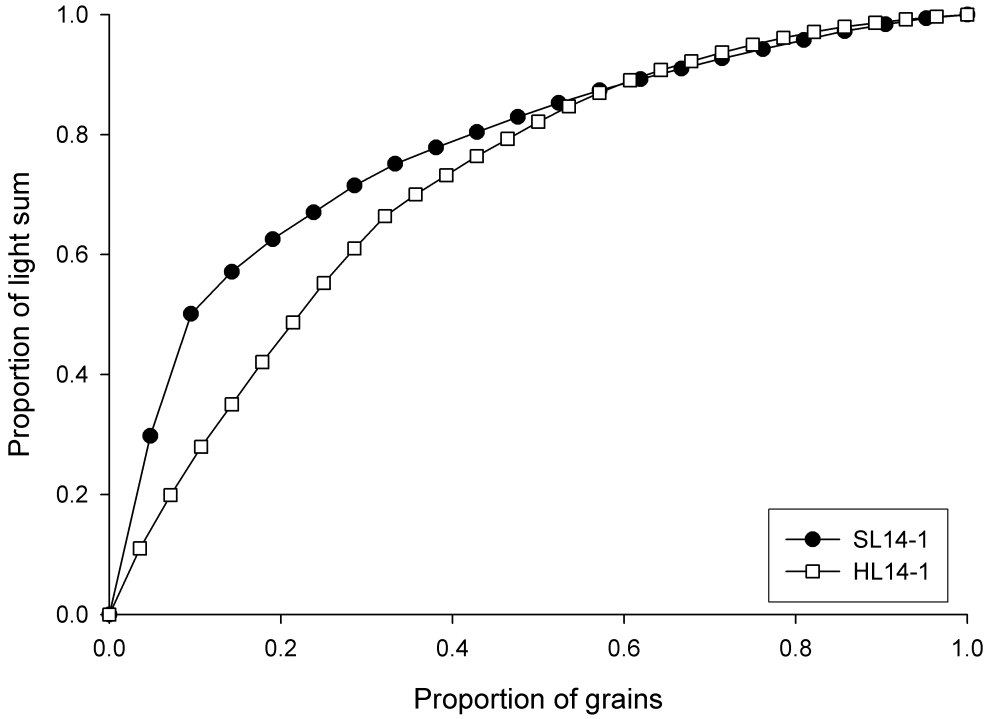

Figure S5: pIRIR$_{225}$ single grain brightness distributions for samples SL14-1 and HL14-1.

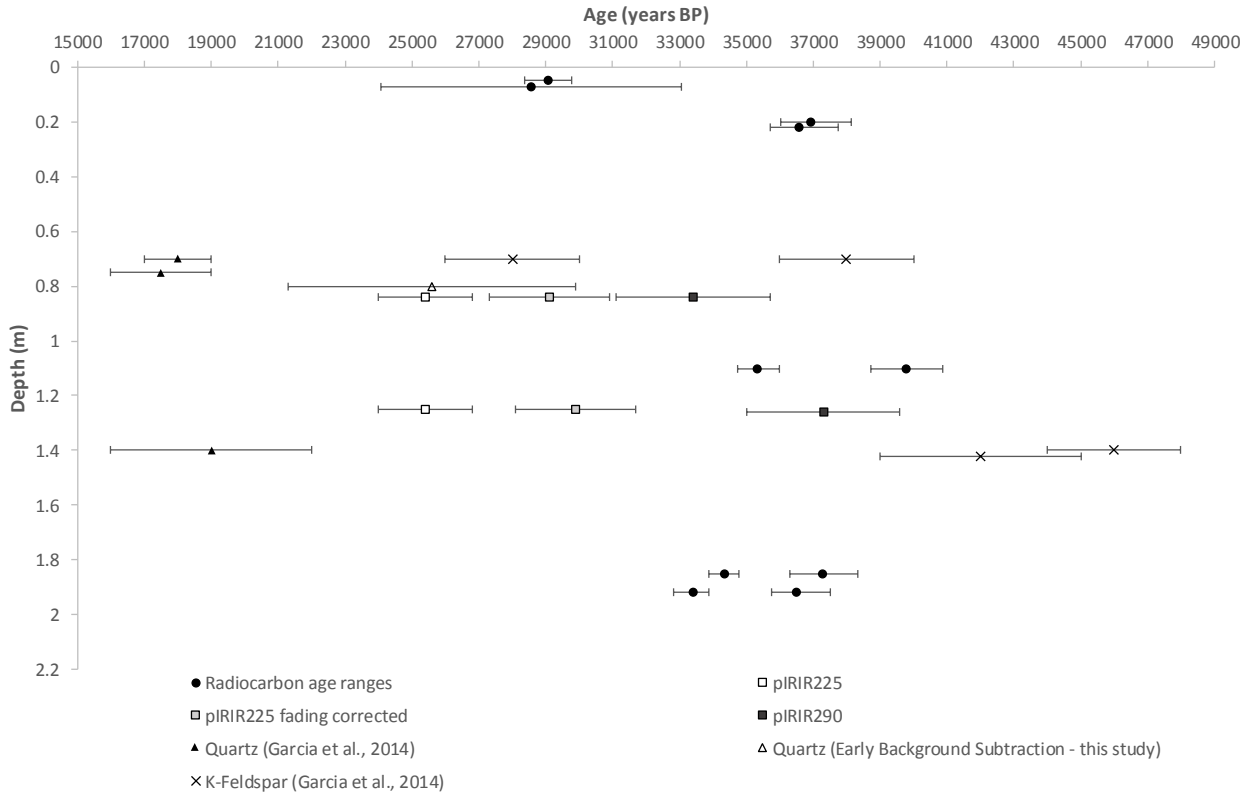

474

475 **Figure S6:** Compared age estimates for the Harper Lake Mountain View Hill site, plotted by depth,
476 including the post-IR IRSL and quartz OSL ages from this study, the MAAD IRSL, quartz OSL ages and
477 calibrated radiocarbon ages from Garcia et al. (2014), and the calibrated radiocarbon ages reported
478 in Meek (1999). The two upper-most radiocarbon samples are from Meek (1999) and have been
479 assigned arbitrary depths for the purposes of illustration.

480

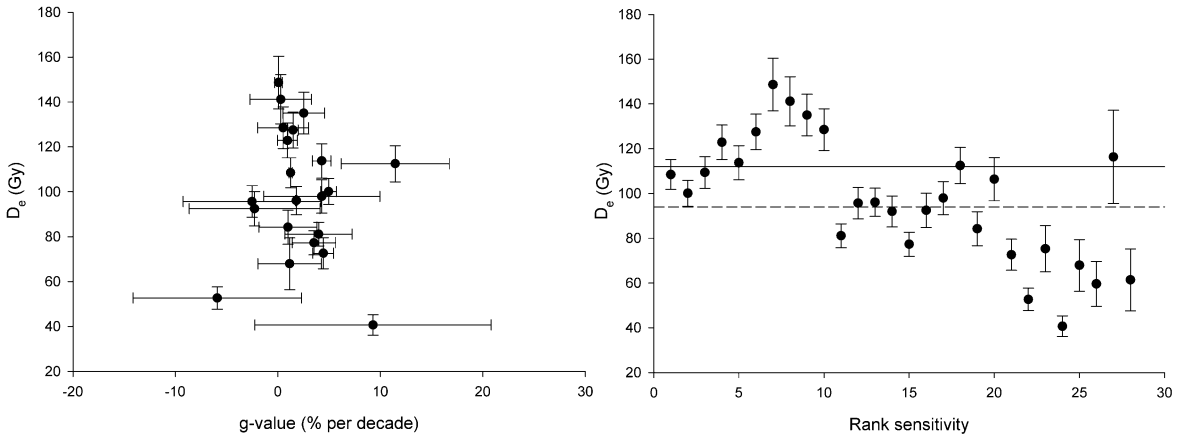

481

482 **Figure S7**: Left: The relationship between individual grain $pIRIR_{225}$ fading rates and single grain D_e for
483 sample HL14-1. Right: Single grain equivalent doses plotted by rank sensitivity (following Rhodes,
484 2015) for HL14-1. The dashed line is the CAM D_e for all grains and the solid line the CAM D_e for the
485 brightest 50% of grains (112 ± 6 Gy).

References

Aitken, M.J 1985. Thermoluminescence Dating. Academic Press, 370p

Garcia, A.L., Knott, J.R., Mahan, S.A., Bright, J. 2014. Geochronology and paleoenvironment of pluvial Harper Lake, Mojave Desert, California, USA. Quaternary Research 81, 305-317.

Guérin, G., Mercier, N., Adamiec, G. 2011. Dose-rate conversion factors: update. Ancient TL 29, 5-8.

Huntley, D.J., Baril D.J. 1997. The K content of the K-feldspars being measured in optical dating or in thermoluminescence dating. Ancient TL 15, 11–13

Huntley, D.J., Hancock, R.G.V. 2001. The Rb contents of the K-feldspars being measured in optical dating. Ancient TL 19, 43–46

Lawson, M.J., Roder, B.J., Stang, D.M., Rhodes, E.J. 2012. OSL and IRSL characteristics of quartz and feldspar from southern California, USA. Radiation Measurements 47, 830-836.

Meek, N. 1999. New discoveries about the Late Wisconsinan history of the late Mojave River system. San Bernadino County Museum Association Quarterly 46, 113-117.

Mejdahl, V. 1979 Thermoluminescence dating: beta-dose attenuation in quartz grains. Archaeometry 21, 61-72.

Owen, L.A., Bright, J., Finkel, R.C., Jaiswal, M.K., Kaufman D.S., Mahan, S., Radtke, U., Schneider J.S., Sharp, W., Singhvi, A.K., Warren, C. 2007. Numerical dating of a Late Quaternary spit-shoreline complex at the northern end of Silver Lake playa, Mojave Desert, California: A comparison of the applicability of radiocarbon, luminescence, terrestrial cosmogenic nuclide, electron spin resonance, U-series and amino acid racemization methods. Quaternary International 166, 87-110.

Prescott, J.R., Hutton, J.T. 1994. Cosmic ray contributions to dose rates for luminescence and ESR dating: Large depths and long-term time variations. Radiation Measurements 23, 497-500.

Readhead, M.L., 2002. Absorbed dose fraction for ^{87}Rb beta particles. Ancient TL 20, 25-29.

Reimer, P.J., Bard, E., Bayliss, A., Beck, J.W., Blackwell, P.G., Ramsey, C.B., Buck, C.E., Cheng, H., Edwards, R.L., Friedrich, M. Grootes, P.M. 2013. IntCal13 and Marine13 radiocarbon age calibration curves 0–50,000 years cal BP. Radiocarbon 55, 1869-1887.

Rhodes, E.J. 2015. Dating sediments using potassium feldspar single-grain IRSL: initial methodological considerations. Quaternary International 362, 14-22.

Stuiver, M. Reimer, P.J., 1993. Extended ^{14}C data base and revised CALIB 3.0 ^{14}C age calibration program. Radiocarbon 35, 215-230.

Vermeesch, P. 2009. RadialPlotter: a Java application for fission track, luminescence and other radial plots. Radiation Measurements 44, 409-410